A direct method of parameter estimation for steady state flow in heterogeneous aquifers with unknown boundary conditions

J. Irsa[1] and Y. Zhang[1]

Received 14 December 2011; revised 23 July 2012; accepted 3 August 2012; published 19 September 2012.

[1] We propose a novel direct method for estimating steady state hydrogeological model parameters and model state variables in an aquifer where boundary conditions are unknown. The method is adapted from a recently developed potential theory technique for solving general inverse/reconstruction problems. Unlike many inverse techniques used for groundwater model calibration, the new method is not based on fitting and optimizing an objective function, which usually requires forward simulation and iterative parameter updates. Instead, it directly incorporates noisy observed data (hydraulic heads and flow rates) at the measurement points in a single step, without solving a boundary value problem. The new method is computationally efficient and is robust to the presence of observation errors. It has been tested on two-dimensional groundwater flow problems with regular and irregular geometries, different heterogeneity patterns, variances of heterogeneity, and error magnitudes. In all cases, parameters (hydraulic conductivities) converge to the correct or expected values and are thus unique, based on which heads and flow fields are constructed directly via a set of analytical expressions. Accurate boundary conditions are then inferred from these fields. The accuracy of the direct method also improves with increasing amount of observed data, lower measurement errors, and grid refinement. Under natural flow (i.e., no pumping), the direct method yields an equivalent conductivity of the aquifer, suggesting that the method can be used as an inexpensive characterization tool with which both aquifer parameters and aquifer boundary conditions can be inferred.

Citation: Irsa, J., and Y. Zhang (2012), A direct method of parameter estimation for steady state flow in heterogeneous aquifers with unknown boundary conditions, *Water Resour. Res.*, *48*, W09526, doi:10.1029/2011WR011756.

1. Introduction

[2] In many physical sciences we have surveyed, parameter estimation studies have focused on the indirect inverse method solving a boundary value problem (BVP) to optimize an objective function, e.g., measurement-to-model misfits. Such approaches satisfy the known physical and mathematical constraints, are easily adaptable, and have proven to be robust and efficient in many applications. However, solution of the BVP requires the prescription of boundary conditions (BCs) which are often unknown. In nonlinear problems, parameter estimation via the indirect method is often an iterative procedure involving repeated simulations of the BVP, a computationally demanding task when the model size is large. Though both model parameters and model BCs can be modified/updated during iterations, the inverse problem can be ill posed, e.g., instability, nonuniqueness, and failure to converge. These issues can be addressed by providing additional (independent) constraints in the form of supplemental or prior information on parameters. However, BVP domain is often a cutout region where the BCs can be highly discontinuous, causing convergence issues. Furthermore, an infinite number of BCs may provide the same solution at the same observation points, thus the inferred BCs are generally nonunique.

[3] The indirect inverse method is extensively investigated in hydrogeology (see reviews by, e.g., *Yeh* [1986], *Ginn and Cushman* [1990], *McLaughlin and Townley* [1996], *de Marsily et al.* [2000], *Carrera et al.* [2005], *Vrugt et al.* [2008a]). To address ill-posedness, a variety of approaches have been proposed, e.g., imposing parameter bounds or parameter lumping [*Hill and Tiedeman*, 2007], regularization [*Cooley*, 1982, 1983; *Carrera and Neuman*, 1986a; *Kitanidis*, 2012], sample network design [*Delhomme*, 1978; *Wagner*, 1995; *Asefa et al.*, 2004; *Janssen et al.*, 2008], reducing model structure error [*Doherty and Welter*, 2010], adopting a highly parameterized or geostatistical formulation [*Zimmerman et al.*, 1998; *Hunt et al.*, 2007; *Tonkin and Doherty*, 2009; *Liu and Kitanidis*, 2011], incorporating static geologic data [*McKenna and Poeter*, 1995; *Sun et al.*, 1995; *Tsou et al.*, 2006], and utilizing auxiliary data such as solute concentration [*Gailey et al.*, 1991; *Medina and Carrera*, 1996; *Anderman et al.*, 1996; *Weiss and Smith*, 1998a], geophysical measurements [*Hyndman et al.*, 1994; *Day-Lewis et al.*, 2006; *Ronayne et al.*, 2008; *Camporese et al.*, 2011], and temperature [*Woodbury and Smith*, 1988;

[1]Department of Geology and Geophysics, University of Wyoming, Laramie, Wyoming, USA.

Corresponding author: J. Irsa, Department of Geology and Geophysics, University of Wyoming, Laramie, WY 82071, USA. (jirsa@uwyo.edu)

Bravo et al., 2002; *Anderson*, 2005]. Moreover, to enhance computational efficiency in calculating sensitivities for the gradient-based (local) methods, adjoint state techniques are developed [*Sun and Yeh*, 1985; *Carrera and Neuman*, 1986b; *Liu and Kitanidis*, 2011]. To enhance robustness in optimizing the objective function, different search algorithms are proposed, including global methods that are not gradient based [*Wang and Zheng*, 1996; *Morshed and Kaluarachchi*, 1998; *Vrugt et al.*, 2008b; *Keating et al.*, 2010]. Instability due to overparameterization is usually addressed by regularization (e.g., parameter bounds, prior information, smoothing, zonation) [*Sun and Yeh*, 1985; *Eppstein and Dougherty*, 1996; *McLaughlin and Townley*, 1996; *Capilla et al.*, 1997; *Weiss and Smith*, 1998b]. In transient or strongly nonlinear cases, a variety of data assimilation techniques have also been developed [*Eppstein and Dougherty*, 1996; *Zhu and Yeh*, 2005; *Chen and Zhang*, 2006; *Liu et al.*, 2008].

[4] Direct methods can also be used to solve the inverse problem. The direct methods are mathematically straightforward and computationally efficient, though their use has not been widely adopted due to instability in the estimated parameters when the observed data are corrupted by noise. In hydrogeology, initial attempts were made to directly determine transmissibility from streamlines by inverting the flow equation along these lines, though the method was found sensitive to measurement errors [*Nelson*, 1960, 1961, 1968]. Though parameter oscillations can be controlled by imposing bounds on the observation errors [*Kleinecke*, 1971], solutions are often unreliable. Other direct formulations, for example, the direct matrix method, create a set of superdeterminate algebraic equations from discretizing the BVP [*Neuman*, 1973; *Sagar et al.*, 1975]. In a two-dimensional problem, when random noise was added to the observed data, this method was found accurate when the parameter dimension was small [*Yeh et al.*, 1983]. *Sun* [1994] further stated that the necessary condition for parameter identifiability is that the number of parameters is smaller than the number of the observation data. In addition many direct formulations require that state variables at measurement points be interpolated to all grid nodes, thus inversion results are influenced by not only the measurement error but also the interpolation error. Another means of controlling instability is to assume that transmissibility satisfies a Cauchy criterion [*Frind and Pinder*, 1973], although the solution can be sensitive to the degree of approximation in the finite element shape functions.

[5] Recently, a new potential theory technique is being developed for solving general inverse/reconstruction problems with an efficient direct method, where errors in measurements do not generally cause stability issues even in certain cases when the systems are ill posed. The method, referred to as stress trajectories element method, has been applied to solid mechanics and geophysics problems with excellent convergence behaviors. Modifications of this method were also proposed for other applications, yielding unique and stable parameters that are also robust to the presence of observation errors [*Irsa and Galybin*, 2010; *Galybin and Irsa*, 2010; *Irsa*, 2011]. The new method consists of discretizing the problem domain into elements where a state variable is approximated with a function satisfying the governing equation a priori, i.e., the Trefftz method [*Trefftz*, 1926] (an English translation is found in *Maunder* [2003]). It does not rely on formulating superdeterminate equations, thus the number of parameters is not constrained by the number of state variables. It directly incorporates the state variables at the observation points without the need for interpolation or iterations. Using smooth Laplace's solution with unknown coefficients, the method in effect imposes a form of regularization: the coefficients are estimated by "bending" the approximate solution toward the true solution, following the observations with its weights. Unlike the existing indirect and direct methods, the new method does not discretize a BVP, thus a priori knowledge of the BCs is not required. Nor does it attempt to fit BCs to observations during inversion, obviating the nonuniqueness issue. In a single step (i.e., single matrix solve), model parameters and model state variables are simultaneously estimated from which BCs of the modeled region can be inferred. The method is thus computationally efficient.

[6] In this study, steady state groundwater flow in a homogeneous and isotropic aquifer is first investigated. Hydraulic head of each element is approximated by a function satisfying the Laplace's equation and Darcy flux is obtained from differentiating the head. The unknown hydraulic conductivity (K) is estimated together with parameters of the head and flux functions. The method is then extended to the study of a heterogeneous isotropic aquifer characterized by different hydrofacies zones. To ensure head and flux continuity at element boundaries, a collocation technique is used: elements within one hydrofacies assume continuous heads and fluxes in all directions, where elements separated by a material interface assume continuity in head and continuity of the normal fluxes. The inversion problem is thus stated with correct physical constraints, with three advantages derived from the direct formulation: (1) model fits the data directly and there is no need to fit an objective function; (2) besides measurement error, numerical discretization is the only source of error, convergence is assured when collocation error decreases with increasing number of elements; (3) element shape is flexible, since nodal connection is not needed in evaluating the fluxes. Given observed hydraulic head data, the direct method can uniquely determine the head and flow fields as well as the BCs. However, to also obtain the parameters (hydraulic conductivity), at least one flow rate measurement is necessary. Although direct flow rate measurement is not as frequently available as the head data, recent advancements in field techniques have made such measurements more readily available [*Leap and Kaplan*, 1988, *Bayless et al.*, 2011; *Devlin et al.*, 2012]. In the following sections, nonuniqueness in fitting BCs for general inversion is discussed first. Then the new direct method is described and demonstrated with several groundwater reconstruction problems. Strength and limitation of the method are then discussed, before future research is indicated.

2. Nonuniqueness in Fitting Boundary Conditions to a Steady State Problem

[7] Most existing methods utilize the solution of a BVP with prescribed BCs which, along with the parameters of the model, can be modified and updated during inversion. However, BCs fitted by such procedure can suffer nonuniqueness, the severity of which depends on the quantity and quality of the observed data. When data quantity/quality is high, the nonuniqueness is less pronounced, although

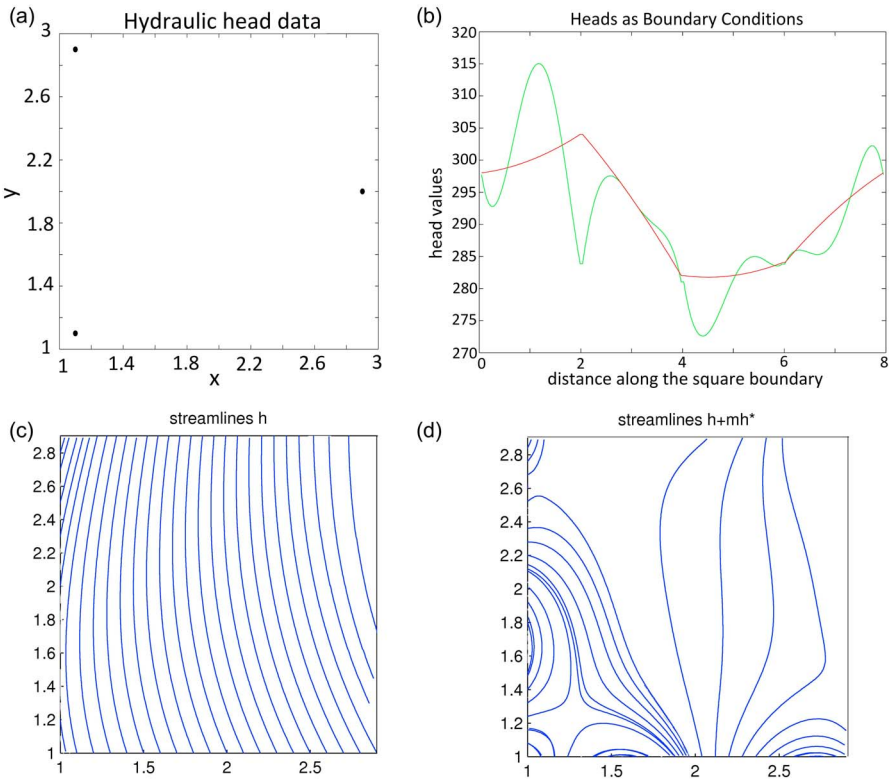

Figure 1. Nonuniqueness in fitting BC in a 2-D homogeneous and isotropic aquifer within a square region [1,1]–[3,3]. (a) Observation data: three heads and one flow rate at the right boundary. (b) Two different Dirichlet BCs. (c and d) Streamlines driven by each BC.

there still exists an infinite number of BCs providing solutions that satisfy the observed data and prior information. Here we illustrate this problem by a two-dimensional (2-D) example of steady state groundwater flow in a homogeneous isotropic aquifer for which hydraulic head satisfies the Laplace's equation: $\nabla^2 h = 0$. Solution of this equation is a harmonic function, which is related to a complex valued holomorphic function: $W(z)$; $z = x + iy$; $z \in C$.

[8] $W(z)$ has real and imaginary parts, both of which are harmonic functions. In some applications the imaginary part (complex conjugate harmonic function to the real part) has physical meanings which can be useful to recover. However, at this point we are only interested in the real part. Let the solution of the Laplace's equation be expressed as

$$h(x,y) = \mathrm{Re}[W(z)], \tag{1}$$

where Re stands for the real part. $W(z)$ can be, for instance, a polynomial:

$$W(z) = \sum_{k=0}^{n} a_k z^k \tag{2}$$

where a_k is a complex parameter and z is a complex variable. Next, we assume that there exist N observed heads at locations $z_j = x_j + iy_j$, $j = 1, \ldots, N$, which can be directly sampled from the solution. Given the solution, we can substitute any boundary points into equation (1) to obtain a set of Dirichlet BCs. Now, let's introduce an arbitrary holomorphic function $W^*(z - z_j)$ with its roots placed at the observation points (for the sake of simplicity it is also assumed a polynomial):

$$W^*(z - z_j) = \prod_{k=1}^{r} b_k (z - z_j)^k, \begin{cases} r = N, j = k \\ r > N, j \in \{1, \ldots N\} \end{cases}, \tag{3}$$

where b_k is a complex parameter. The real part of W^* is

$$h^*(x,y) = \mathrm{Re}\left[W^*(z - z_j)\right], \tag{4}$$

h^* satisfies the Laplace's equation, and its roots are placed exactly at the observed points z_j, thus h^* is a solution of the same problem. Let us introduce an additional arbitrary parameter m. Due to linearity of the Laplace's equation, $h + mh^*(x, y)$ is also a solution. Substitution of the observed data coordinates z_j into the superposition does not affect the observed data (h) since $mh^*(x,y)$ vanishes at these points. For any $r \geq N$ and any m, $h^*(x,y)$ always vanishes at the data locations. For any b_k, r, and m, there exist an infinite number of solutions satisfying the observed heads and each of the infinite solutions has a different set of BCs that can be obtained by substituting z at the boundary. In other words, there exists an infinite number of BCs satisfying the observed heads, with associated infinite solutions describing different flow fields.

[9] One may assume, as it is commonly assumed, that by adding flow rate data, the nonuniqueness in fitting the heads can be reduced, and perhaps a unique solution is possible. For example, a flow rate measured along any distance/

contour in the aquifer would impose an additional constraint on the solution. Here, however, we demonstrate using a 2-D square model with a constant K that adding flow rate data cannot ensure uniqueness of the solution. In this case, a flow rate Q_x [L^2/T] along the y axis (−1 to 1) can be used to modify the arbitrary function h^*:

$$Q_x|_y = \int_{-1}^{1} -K\frac{\partial h^*(x,y)}{\partial x}dy = -K\int_{-1}^{1} \mathrm{Re}\frac{\partial W^*(z-z_j)}{\partial z}dy. \quad (5)$$

[10] Equation (5) provides an additional constraint equation leading to one less coefficient, i.e., b_k, $k = 1, \ldots, r-1$. However, an infinite number of b_k satisfies the head solutions. The addition of flow rate does not guarantee a unique solution, but allows for the determination of K, which would remain a free undetermined parameter without the flow rate. To reduce the number of possible solutions, an infinite number of flow rate measurements are needed. With respect to equation (3), this would be r flow rates. With each additional observation, be it head or flow rate, the class of functions (equation (3)) converges toward a unique solution.

[11] Let's illustrate this problem graphically (Figure 1). The solution, $W(z)$, is assumed as a second-order polynomial, with parameters $a_0 = 300$ and $a_1 = a_2 = 1 + i$. The corresponding hydraulic head is $h(x, y) = 300 + x - y - 2xy + (x^2 - y^2)$. Three head data ($N = 3$) are sampled directly from the solution at locations $z \in (1.1 + i1.1; 1.1 + i2.9; 2.9 + i2)$. A flow rate is obtained analytically along the y axis on the right-hand-side boundary (this flow rate could be given anywhere within the domain). The arbitrary function $W^*(z - z_j)$ of equation (3) is introduced with these parameters: $r = N$, $m = 0.4$ and $b_k = 1 + i1.19$. Parameters b_k are uniform and are derived to satisfy the flow rate for a constant K value of 1 (equation (5)). Two different Dirichlet BCs are specified along the model boundary (Figure 1b), leading to different reconstructed flow fields (Figures 1c and 1d), while both solutions honor the same observed data of 3 heads and one flow rate. In this problem, the additional flow rate at the right-hand-side boundary does not lead to a unique estimation of heads along the same boundary (Figure 1b, between distance 2–4), due to an abrupt change in streamlines which significantly changes the flow direction and the interconnected fluxes, while maintaining the same Q_x. In addition, significant change in the flow field occurs in the vicinity of the observed heads, where one would normally expect the highest accuracy in head predictions.

3. New Direct Method

[12] The new direct method provides the best fit to the observed data with stable convergence, without the need for iterations. It is not based on solving a BVP, thus a priori knowledge of the BCs is not necessary. Nor does it attempt to fit BCs to observations, obviating the nonuniqueness issue.

3.1. Background

[13] The new direct method is derived ultimately from the Trefftz method, which superimposes functions that satisfy the governing equations a priori, where the unknown coefficients are determined by minimizing these functions. A similar concept is the Method of Fundamental Solution [*Kupradze and Aleksidze*, 1964], which is mathematically equivalent to the Trefftz method as the number of coefficients of the individual superimposed functions increases to infinity [*Li et al.*, 2010]. Application of the Trefftz method was initially focused on inverse problems, before the current focus on BVP, with both finite element formulations [*Jirousek and Zielinski*, 1997; *Kita and Kamiya*, 1995; *Herrera*, 2000; *Li et al.*, 2008; *Kolodziej and Zielinski*, 2009] and meshless method [*Galybin and Mukhamediev*, 2004].

[14] The new direct method extends from the meshless method of *Galybin and Mukhamediev* [2004], where a discretized approach is adopted to eliminate instabilities characterizing the former method. It thus combines the strengths of the discretization-based approaches and the Trefftz method. Within a problem domain, the new method seeks a solution via a set of specialized collocation points which lie on element interfaces. The technique was initially developed for two-dimensional geophysical problems using the complex variable theory, e.g., determination of stresses in the lithospheric plate from observations on the principal stress directions [*Irsa and Galybin*, 2010]. It was later extended to multiple plates and their interactions to identify stress change in the Earth's crust after an earthquake [*Irsa and Galybin*, 2011b]. A modification of this method led to the determination of heat fluxes from discrete temperature measurements [*Irsa and Galybin*, 2009] and fluid velocity from its trajectories [*Irsa and Galybin*, 2011a]. A three-dimensional version was developed for heat flux reconstruction as well as for determining deformations from discrete dilation data [*Galybin and Irsa*, 2010]. In many such systems, given the nature of the data and their errors, conventional indirect methods often fail to converge. The new method is applicable to any problems described by the potential theory as long as a fundamental solution exits, i.e., a solution can be found that satisfies the governing equations a priori.

3.2. Fundamental Solution

[15] The equations describing 2-D steady state groundwater flow without source/sink are:

$$\begin{aligned} \nabla \cdot (\mathbf{q}) &= 0 \\ \mathbf{q} &= -K(x,y)\nabla h \end{aligned} \quad (6)$$

where ∇ is gradient operator, h is hydraulic head, and $\mathbf{q}$ is Darcy flux. The problem domain can be discretized into elements (or grid cells) where the hydraulic head satisfies the fundamental solution of equation (6). In the case of a homogenous and isotropic aquifer, this solution is a harmonic function in each element. For simplicity, we use the complex valued holomorphic function $W(z)$, whose real part is harmonic, and thus is the fundamental solution of this problem. Here, $W(z)$ is specified as a second-order polynomial:

$$W(z) = \sum_{n=0}^{2} a_n z^n, \quad (7)$$

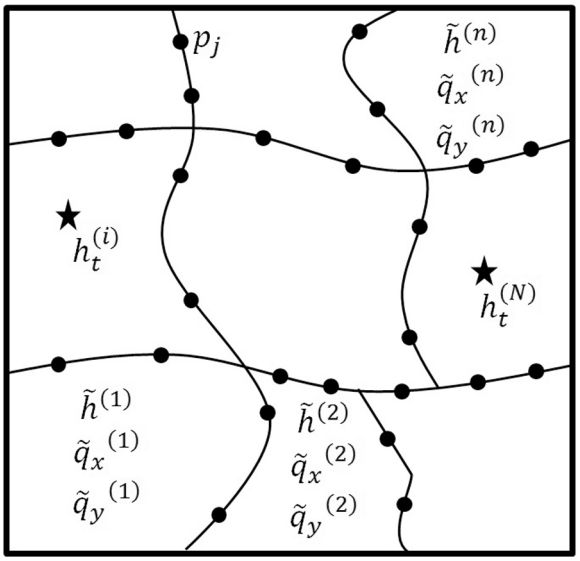

Figure 2. Domain discretization with n elements and a set of collocation points (solid circles). The approximating functions are shown in each element. Stars are the head measurement locations ($t = 1, \ldots, N$).

where $z = x + iy$ and $a_n \in C$. Head and flux of the kth element can then be approximated:

$$\tilde{h}^{(k)}(x,y) = a_{00}^{(k)} + a_{10}^{(k)}x - a_{11}^{(k)}y + a_{20}^{(k)}\left(x^2 - y^2\right) - 2a_{21}^{(k)}xy, \quad (8a)$$

$$\tilde{q}_x^{(k)}(x,y) = -K\left(a_{10}^{(k)} + 2a_{20}^{(k)}x - 2a_{21}^{(k)}y\right), \quad (8b)$$

$$\tilde{q}_y^{(k)}(x,y) = -K\left(a_{11}^{(k)} - 2a_{20}^{(k)}y - 2a_{21}^{(k)}x\right), \quad (8c)$$

where $a_0^{(k)} = a_{00}^{(k)}$; $a_1^{(k)} = a_{10}^{(k)} + ia_{11}^{(k)}$; $a_2^{(k)} = a_{20}^{(k)} + ia_{21}^{(k)}$. For each element, five real-valued unknowns need to be determined. Though the complex variable theory allows for easy adaptation of the fundamental solution to higher orders, it was found that a linear or quadratic approximation is often satisfactory [*Galybin and Irsa*, 2010]. The use of higher-order approximations within elements is permissible, which can lead to coarsened meshes. To simplify our analysis, we restrict ourselves here to the quadratic approximation with numerical convergence tests.

3.3. Continuity

[16] Having the fundamental solutions described for each element (equation (8)), the solution must also satisfy the governing equation globally. This is accomplished by minimizing a residual function on a set of collocation points p_j which lie on the boundary between adjacent elements (Figure 2). This minimization forces the residuals to vanish at each point:

$$\int R(\Gamma_j)\delta(p_j - \varepsilon)d\Gamma_j = 0, j = 1, \ldots, m_c, \quad (9)$$

where m_c is the total number of element boundaries, $R(\Gamma_j)$ is the residual of an approximating function at the jth boundary, and $\delta(p_j - \varepsilon)$ is the Dirac delta weighting function. In general, continuity along element boundaries is without errors, thus $\lim_{\varepsilon\to 0}\delta(p_j - \varepsilon) = 1$. However, the new direct method solves an overdetermined problem, thus the weighting function on the element boundaries can be reduced to $\delta(p_j - \varepsilon) < 1$, reflecting equal weighting of the observations and continuity at the collocation points. This results in a well-posed system matrix, leading to faster convergence during its solution. Equation (9) gives an average residual across an element boundary, which is replaced in the discrete case by summation of the residuals at the collocation points (2 are shown here). The residual $R(\Gamma_j)$ is then replaced by the residual $R(p_j)$ at the collocation point. At data locations, equation (9) is also formulated, where $\delta(p_j - \varepsilon)$ represents the measurement error and $R(\Gamma_j)$ is replaced with residuals at the data points $R(t_j)$, where t_j is the jth data point. The formulation of the data residuals is the same if the observation data lie on the Dirichlet, Neumann, or mixed boundaries.

[17] In this study, equation (9) is used in analyzing homogenous and heterogeneous aquifers. However, the hydraulic head approximation function (equation (8a)) is modified for the heterogeneous aquifers.

4. Algorithms

[18] The study estimates 2-D steady state hydrogeological model parameters, model state variables, and the unknown model BCs for (i) a homogenous aquifer, (ii) single (equivalent) K determination for heterogeneous and stratified aquifers, and (iii) heterogeneous aquifer where prior information on K is available. In the last case, prior information is in the form of hydrofacies zonation and K relationships between adjacent hydrofacies zones. Individual measurement errors are specified on the observed data with a weighting scheme reflecting an assumed magnitude of the errors.

4.1. Homogeneous Isotropic Aquifer

[19] Conductivity is a scalar constant throughout the solution domain. Three residuals are evaluated: hydraulic head, Darcy flux x component, and Darcy flux y component. To enforce continuity across element boundaries, the head residual can be written at each element boundary as

$$\delta(p_j - \varepsilon)R_h(p_j) = \delta(p_j - \varepsilon)\left(K\tilde{h}^{(k)}(x_j,y_j) - K\tilde{h}^{(l)}(x_j,y_j)\right) = 0, j = 1, \ldots, m \quad (10)$$

where k and l are elements adjacent to p_j, and m is the number of collocation points on each boundary (here $m = 2$). The residual is multiplied by K in order to extract the conductivity value from the solution.

[20] For the flux residuals, continuity is also enforced:

$$\delta(p_j - \varepsilon)R_{qx}(p_j) = \delta(p_j - \varepsilon)\left(\tilde{q}_x^{(k)}(x_j,y_j) - \tilde{q}_x^{(l)}(x_j,y_j)\right) = 0, j = 1, \ldots, m \quad (11a)$$

$$\delta(p_j - \varepsilon)R_{qy}(p_j) = \delta(p_j - \varepsilon)\left(\tilde{q}_y^{(k)}(x_j,y_j) - \tilde{q}_y^{(l)}(x_j,y_j)\right) = 0, j = 1, \ldots, m \quad (11b)$$

Thus at each collocation point p_j, 3 equations enforce the condition of continuity. By writing equations (10) and (11)

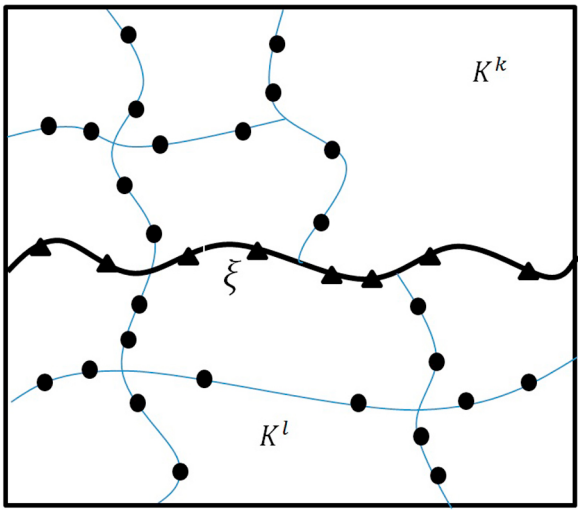

Figure 3. Schematics of a domain with two hydrofacies separated by interface ξ. Domain is discretized with n elements and a set of collocation points (solid circles at element boundaries internal to a hydrofacies; triangles at the interface).

at all collocation points, we obtain a system of linear algebraic equations. A domain of n elements will yield $5n$ unknowns: $\{Ka_{00}^{(1)}, Ka_{10}^{(1)}, Ka_{11}^{(1)}, Ka_{20}^{(1)}, Ka_{21}^{(1)}, \ldots, Ka_{00}^{(n)}, Ka_{10}^{(n)}, Ka_{11}^{(n)}, Ka_{20}^{(n)}, Ka_{21}^{(n)}\}$.

[21] After enforcing continuity at every collocation point, the approximation needs to further honor the observed heads. For element k, where the tth observed head lies, we have: $h_t(x_t, y_t) = \tilde{h}^{(k)}(x_t, y_t)$. Multiplying by K,

$$Kh_t(x_t, y_t) = K\tilde{h}^{(k)}(x_t, y_t) \tag{12}$$

where (x_t, y_t) is the coordinate of the observed head $h_t(x_t, y_t)$. However, $h_t(x_t, y_t)$ contains measurement errors, thus head residual for element k is weighted by the inverse of the error variance $\delta(p_j - \varepsilon)$ for observation t:

$$\delta(p_t - \varepsilon)\left(K\tilde{h}^{(k)}(x_t, y_t) - Kh_t(x_t, y_t)\right) = 0,\ t = 1, \ldots, N, \tag{13}$$

where N is the number of head measurements. The right-hand sides of equation (10), (11), and (13) are zeros, thus the solution of the above system is trivial. To estimate K uniquely, at least one flow rate measurement is needed. Equations relating to the flow rates are introduced below, where the right-hand sides present the weighted flow rate measurements and the left-hand sides describe the integration of groundwater fluxes along arbitrary contours where flow rates are measured. For example, along a vertical line parallel to the y axis (crossing elements e to f), flow rate can be approximated as

$$\begin{aligned}\tilde{Q}_y(x, y) &= \sum_{k=e}^{f}\left[\int_0^{dy^{(k)}} \tilde{q}_y^{(k)} dy\right] \\ &= \sum_{k=e}^{f}\left[-Ka_{11}^{(k)} dy^{(k)} + Ka_{20}^{(k)} dy^{(k)^2} + 2Ka_{21}^{(k)} x dy^{(k)}\right],\end{aligned} \tag{14}$$

where x is fixed and $dy^{(k)}$ is length of the kth element along elements e to f. The flow rate is satisfied analytically and there is no need for collocation points on this line. To further account for flow rate measurement error, the residual equation (equation (9)) for the flow rate takes this form at each flow rate measurement location:

$$\delta(p - \varepsilon)(\tilde{Q}_y(x, y) = \delta(p - \varepsilon)Q_y. \tag{15}$$

The addition of equation (15) yields a nontrivial solution, leading to unique estimation of K. The final equation system consists of equations (10), (11), (13) and (15):

$$\mathbf{Ax} = \mathbf{b}. \tag{16}$$

where $\boldsymbol{A}$ is a sparse matrix (r x s): three diagonals populating most of the system representing continuities, and sporadically populated entries representing observations. Here r is the number of equations, including $3m_c m$ continuity equations, N observed head equations, and g flow rate equations ($r = 3m_c m + N + g$). Here s is the number of unknowns ($s = 5n + 1$), $\boldsymbol{x}$ is the solution vector of size s, $\mathbf{x} \in \{Ka_{00}^{(1)}, Ka_{10}^{(1)}, Ka_{11}^{(1)}, Ka_{20}^{(1)}, Ka_{21}^{(1)}, \ldots, Ka_{00}^{(n)}, Ka_{10}^{(n)}, Ka_{11}^{(n)}, Ka_{20}^{(n)}, Ka_{21}^{(n)}, K\}$, and $\mathbf{b}$ is of size r, consisting of all zeros, except the g nonzero flow rates. For a detailed formation of the matrix, see Appendix in *Irsa and Galybin* [2010]. The system is overdetermined, thus we are solving a least squares solution, where the approximating functions with the unknown coefficients are minimized to the observations with the assigned weights. Because $\boldsymbol{A}$ is generally not ill posed, it can be solved directly:

$$\mathbf{x} = inv(\mathbf{A}^T\mathbf{A})\mathbf{A}^T\mathbf{b}. \tag{17}$$

Should the system be large, an iterative algorithm is preferred, e.g., LSQR algorithm [*Paige and Saunders*, 1982]. After solving for K and the coefficients $a^{(k)}$, head and flux functions in each element are obtained from equation (8). In this study, we use a single flow rate measurement ($g = 1$) which is found sufficient for uniquely identifying K.

4.2. Heterogeneous Isotropic Aquifer

[22] To solve the heterogeneous isotropic aquifer (Figure 3), the previous method is modified, where hydrofacies geometry and prior information on conductivity are needed:

$$K^{(g)} = n_g K^{(g+1)},\ g = 1, \ldots, M - 1, \tag{18}$$

where M is number of hydrofacies and n_g is a known constant describing the relation between K values of adjacent facies.

[23] The heterogeneous aquifer is evaluated using the same set of residual expressions (equation (9)); however, two types of continuities are enforced. For those element boundaries lying within a single hydrofacies, the residual equations remain the same, i.e., equation (10) and (11). At element boundaries coinciding with a hydrofacies interface,

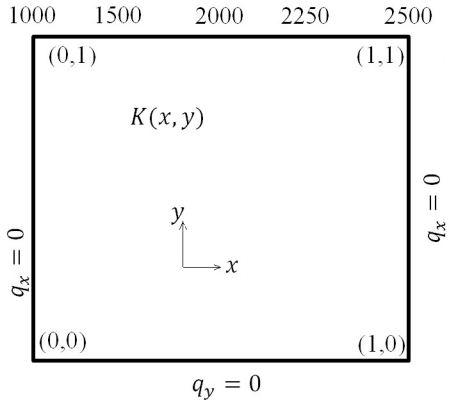

Figure 4. A 2-D flow model used by most of the test examples: no flow on the left, right, and bottom boundaries and heads specified on the top boundary (linearly interpolated between the values). To provide the observation data, the domain is discretized into 20 × 20 FDM block cells.

the head residual equation is multiplied by conductivity of one of the hydrofacies:

$$\delta(p_j-\varepsilon)R_h(p_j)=\delta(p_j-\varepsilon)\left(K^{(k)}\tilde{h}^{(k)}(x_j,y_j)-K^{(k)}\tilde{h}^{(l)}(x_j,y_j)\right)=0, j=1,\ldots,m, \quad (19)$$

where k and l are elements adjacent to p_j on a hydrofacies interface ($K^{(k)}$ and $K^{(l)}$). m is the number of collocation points on the interface. Knowing n_g, equation (18) is substituted into equation (19):

$$\delta(p_j-\varepsilon)R_h(p_j)=\delta(p_j-\varepsilon)\left(K^{(k)}\tilde{h}^{(k)}(x_j,y_j)-n_kK^{(l)}\tilde{h}^{(l)}(x_j,y_j)\right)=0, j=1,\ldots,m. \quad (20)$$

[24] At the hydrofacies interface ξ, continuity of the normal flux is then enforced. The normal flux can be expressed as: $q_n(\xi_j) = q_x(\xi_j)\cos(\alpha_j(\xi_j)) + q_y(\xi_j)\sin(\alpha_j(\xi_j))$, where $\alpha_j(\xi_j)$ is the angle of the normal vector to the interface with respect to x evaluated at ξ_j. Thus, at a collocation point p_j on ξ, the normal flux residual equation is

$$\delta(p_j-\varepsilon)R_{qn}(p_j)=\delta(p_j-\varepsilon)\left(\tilde{q}_n^{(k)}(x_j,y_j)-\tilde{q}_n^{(l)}(x_j,y_j)\right)=0, j=1,\ldots,m. \quad (21)$$

[25] The residual equations for the observed heads are written similarly as in equation (13), with the exception that heads lying in different hydrofacies have different conductivities, thus the K is substituted according to the prior information equation (18):

$$\delta(p_t-\varepsilon)\left(K\tilde{h}^{(k)}(x_t,y_t)-Kh_t(x_t,y_t)\right)=0\begin{cases}(k)\in K^{(k)}\rightarrow K=K^{(k)}\\(k)\notin K^{(k)}\rightarrow K=n_gK^{(k)}\end{cases}, t=1,\ldots,N. \quad (22)$$

Finally, the same flow rate equations, i.e., equation (15), are incorporated.

[26] A system of equations is formed from (10), (11), (20)–(22) and (15). The size of $\boldsymbol{A}$ is (r x s). r is the number of equations, including the continuity equations at element boundaries ($3m_b$) and interfaces ($2m_i$), the observed head equations (N), and g flow rate equations ($r = 3m_b + 2m_i + N + g$), where m_b and m_i is the total number of collocation points on element boundaries and hydrofacies interfaces, respectively. s is number of unknowns ($s = 5n + 1$). $\boldsymbol{x}$ is the solution vector of size s, $\mathbf{x} \in \{Ka_{00}^{(1)}, Ka_{10}^{(1)}, Ka_{11}^{(1)}, Ka_{20}^{(1)}, Ka_{21}^{(1)},\ldots, Ka_{00}^{(n)}, Ka_{10}^{(n)}, Ka_{11}^{(n)}, Ka_{20}^{(n)}, Ka_{21}^{(n)}, K^{(1)}\}$. Only one hydrofacies K is solved; conductivities of the other hydrofacies are obtained from equation (18). **b** is of size r, consisting of all zeros except nonzero flow rates. The system is solved with equation (17).

5. Simulation Examples

[27] Four simulation cases are designed to test the direct method and the proposed algorithms. The observed data are obtained from solving an appropriate BVP using the finite difference method (FDM) and Gaussian Elimination. The first three simulation cases use a problem configuration shown in Figure 4; the associated FDM solves the flow equation on a rectangular grid with 20 × 20 cells. Random errors are imposed on the simulated observed heads, $h_j = h_j^{FDM}\left(1+\frac{\varepsilon}{100}\mu\right), j=1,\ldots,N$; where ε is percent measurement error and $\mu \in (-1,1)$, drawn from a truncated Gaussian distribution by taking $f(x) = ae^{-\frac{(x-b)^2}{2c^2}}$ with parameters $a = 1$, $b = 0$, $c = 1/e$, and cutout values $(-\infty, -1] \cup [1, \infty)$. The one flow rate measurement is assumed error free in this study for all test cases.

[28] The test cases are (a) homogeneous isotropic aquifer; determination of a single K, (b) heterogeneous and stratified aquifers; determination of an equivalent K, (c) heterogeneous locally isotropic aquifer; determination of hydrofacies K values, and (d) hypothetical example with irregular aquifer geometry. Results of each case are reconstructed fields of hydraulic head, fluxes, streamlines, and the estimated conductivity values. A percent relative error in the reconstructed head is defined as: $\varepsilon(\%) = \frac{(h_{FDM}-h_{rec})}{h_{FDM}} \times 100\%$, where h_{FDM} are noise-free (true) nodal heads computed for the BVP and h_{rec} is the recovered head (equation (8)) at the same location. Average $\bar{\varepsilon}$ and maximum relative errors $\bar{\varepsilon}_{\max}$ are also computed. In this study, error in the prior model is not considered, though error-based weighting on the prior information equation can be considered in the future. In the following test cases, dimensions for all relevant quantities implicitly assume a consistent set of units (K in m/d, q in m/d, Q in m^2/d), thus the units are not labeled.

5.1. Homogeneous Isotropic Aquifer

5.1.1. 25 + 1 Observations Without Errors

[29] In this example, true $K(x, y) = 1$. Heads are observed at 25 points on a dense 5 × 5 network distributed uniformly in the problem domain. The flow rate measurement (Q_y) is along the right boundary. The direct method uses a coarse grid with 10 × 10 square elements, 4 times coarsening compared to the FDM approximation. Conductivity computed from the direct method is $K = 0.78$, with $|\varepsilon_{\max}| = 2\%$ and $\bar{\varepsilon} = 0.38\%$. The grid resolution is then increased to 30 × 30 square elements, yielding $K = 0.91$ and $\bar{\varepsilon} = 0.2\%$. In both cases, the direct matrix is well conditioned, leading to

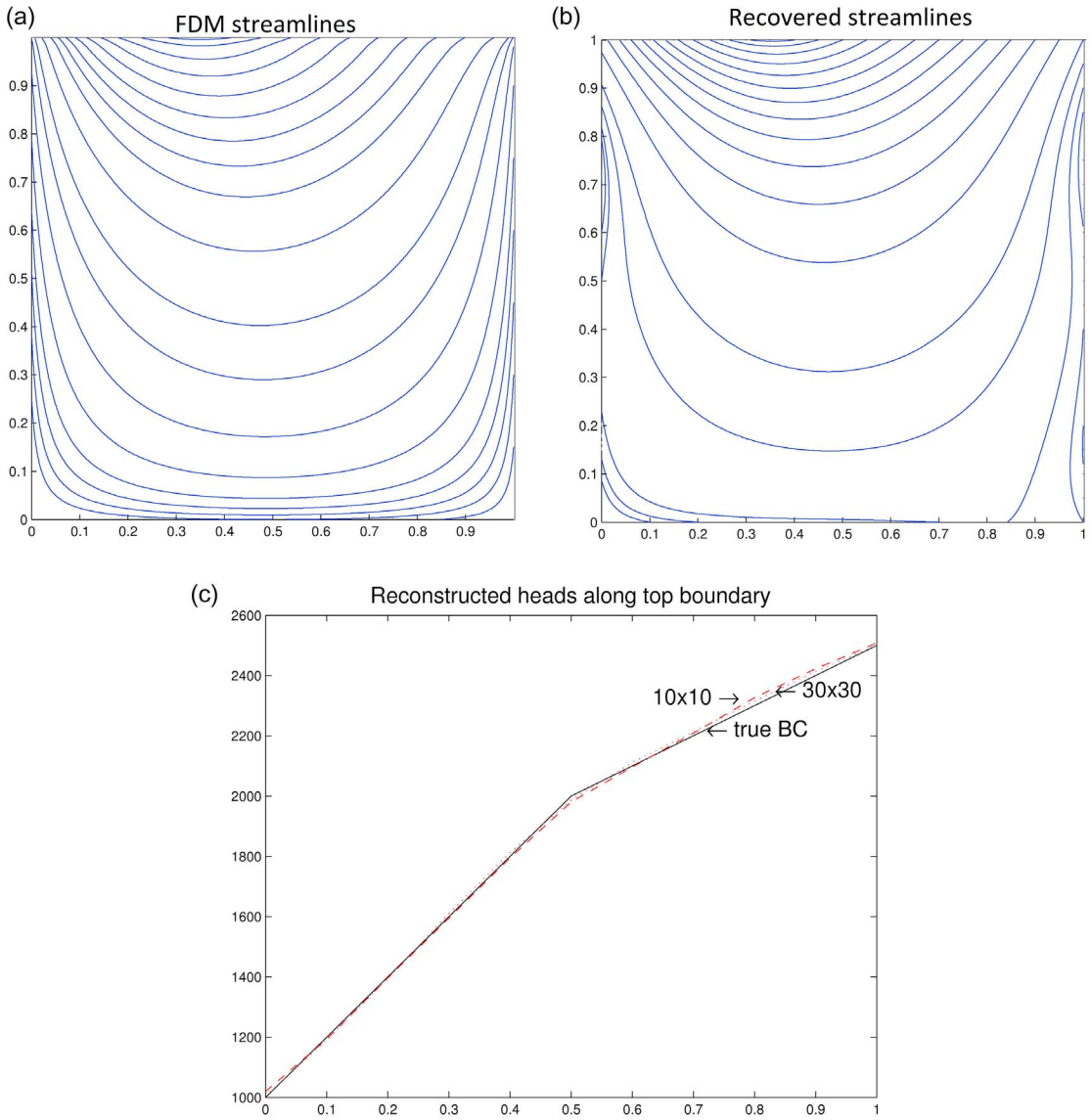

Figure 5. Streamlines from (a) the FDM and (b) the direct method (25 + 1 observed data, 30 × 30 elements). (c) Reconstructed head BCs shown for 10 × 10 (dashed line) and 30 × 30 (dotted line) elements grid. "True BC" is that used by the FDM.

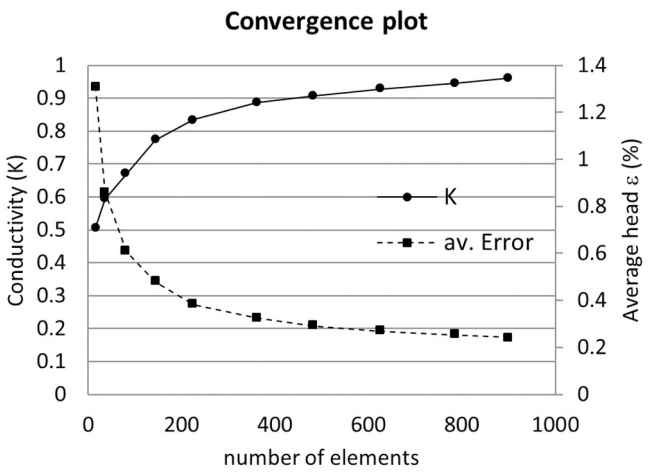

Figure 6. Convergence of K and $\bar{\varepsilon}$ with increased level of discretization based on 15 + 1 observations. True conductivity is $K = 1$.

a stable inversion of the K. In the 30 × 30 case, streamlines are computed from the reconstructed flow field (Figure 5b), which can be used to infer the no-flow condition along the model sides and bottom. Along the model top, the reconstructed head function yields the specified BCs with excellent accuracy (Figure 5c.).

5.1.2. 15 + 1 Observations Without Errors

[30] This example tests the direct method when there are fewer observed data. Heads are measured at locations x = 0.05, 0.47, 0.9, with 5 observation points placed uniformly along each profile. Flow rate Q_y is measured along the right boundary. With a 10 × 10 discretization, we find: $K = 0.75$, $\bar{\varepsilon} = 0.54\%$, $|\varepsilon_{\max}| = 5.6\%$. The discretization is then refined (Figure 6). Conductivity converges toward the correct value asymptotically (Figure 6), e.g., $K = 0.5$ for a 2 × 2 grid; $K = 0.96$ for a 30 × 30 grid. The average head error ($\bar{\varepsilon}$) also diminishes with grid refinement.

5.1.3. 15 + 1 Observations With Data Errors

[31] The previous example is repeated but the observed data are subject to measurement errors which are created with a Gaussian random number generator. According to *Hill and Tiedeman* [2007], errors assigned to one kind of observation data may have equal variance, thus it is common to set the observed head weights to 1. In this example, a standard deviation (*std*) is set at 9.5 to model the head error (absolute measurement error ∼±1% of the total head variation). A 10 × 10 grid results in $K = 0.73$, $\bar{\varepsilon} = 0.76\%$, and $|\varepsilon_{\max}| = 7.3\%$. For a 30 × 30 grid, given the same measurement errors, $K = 0.98$, and the reconstructed head errors are accordingly smaller.

[32] To test the stability of the method, higher head errors are then imposed: *std* = 102 (absolute measurement error ∼±10% of the total head variation). For the given boundary conditions of the test problem, the FDM simulated heads in the bottom half of the domain vary between 1800 and 1930 (Δh = 130), while locally, head measurement errors can reach up to ±200. Using the direct method the reconstructed streamlines in this region change directions (up to 180°), creating vortexes and singularities. Such a situation would not normally be solvable with many inverse methods, but the direct method still gave a stable inverted K of 0.24 (10 × 10 grid), less than 1 order of deviation from the true K.

5.2. Equivalent K

[33] A heterogeneous aquifer can be represented by an equivalent homogenous medium. A well-known analytic solution for layered (equal-thickness) hydrofacies gives an equivalent K as harmonic mean for flow perpendicular to layering and arithmetic mean for flow parallel to layering. Although we do not provide a rigorous proof, the following examples demonstrate that the direct method (section 4.1) leads to the estimation of an equivalent K.

5.2.1. Random ln(K) Map

[34] For a Gaussian distribution of ln(K) without spatial correlation, the analytic equivalent K is the arithmetic mean. A 10 × 10 ln(K) field is created, each K is represented by 4 cells in a 20 × 20 FDM grid. The same BCs are used to drive the flow (Figure 4). Observation errors are assumed zero. A Gaussian ln(K) field is generated with a mean of 1 and a *std* of 0.1 (arithmetic mean and *std* of K are 2.7 and 0.3, respectively). First, dense data are used, i.e., 25 observed heads and one flow rate. With a 10 × 10 grid, the estimated $K = 2.0$; with a 30 × 30 grid, $K = 2.4$, approaching the arithmetic mean (2.7). Then, fewer data are used, i.e., 15 heads and one flow rate, which yields: $K = 2.0$ (10 × 10 grid) and 2.6 (30 × 30 grid). Clearly, this particular estimation is insensitive to the amount of the observed data.

[35] The Gaussian ln(K) field is then scaled to a higher variance (mean $K = 3.2$ and *std* = 1.0), while such errors are extreme, the method still estimates a reasonable value: $K = 1.9$ (10 × 10 grid) and $K = 2.2$ (30 × 30 grid). The convergence to the mean value is slower compared to when ln(K) variance is low. This behavior is similar to that observed for the homogeneous isotropic case with nonzero observed head errors. In a certain sense, ln(K) variance may be viewed as a source of error for the observed heads. Note, that in the FDM solution itself, discretization error, interblock conductivity weighting scheme, and the solution method also introduce errors to the FDM and thus also to the direct method. While refinement in FDM and better solution technique may lead to more accurate results and thus better estimation of K in the direct method, this topic is not investigated in this study.

5.2.2. Flow Parallel to Stratification

[36] When flow is parallel to hydrofacies stratification and zones are of equal thickness, the analytic equivalent K is the arithmetic mean (Figure 7a). In this problem a uniform flow is driven by constant heads (1000 at the top and 100 at the bottom), while the sides are no flow. For this BCs and 3 known K values ($K_1 = 1$, $K_2 = 10$ and $K_3 = 100$; arithmetic mean is 37.0), 18 heads are sampled from the FDM solution at: $x = 0.05$, 0.47, 0.9 (6 observations uniformly placed across each profile). A flow rate Q_y is sampled along a horizontal line at $y = 0.5$ crossing all zones. Random error is added to all the observed heads with *std* = 13 (measurement error up to ±3% of the total head variation). For this problem with linearly varying heads, results converge immediately to $K = 39.6$ for a grid as small as 2 × 2. The method is also stable at larger errors, such as *std* = 40 (error up to ±10%). In this case, K obtained with a 30 × 30 grid is 34.0.

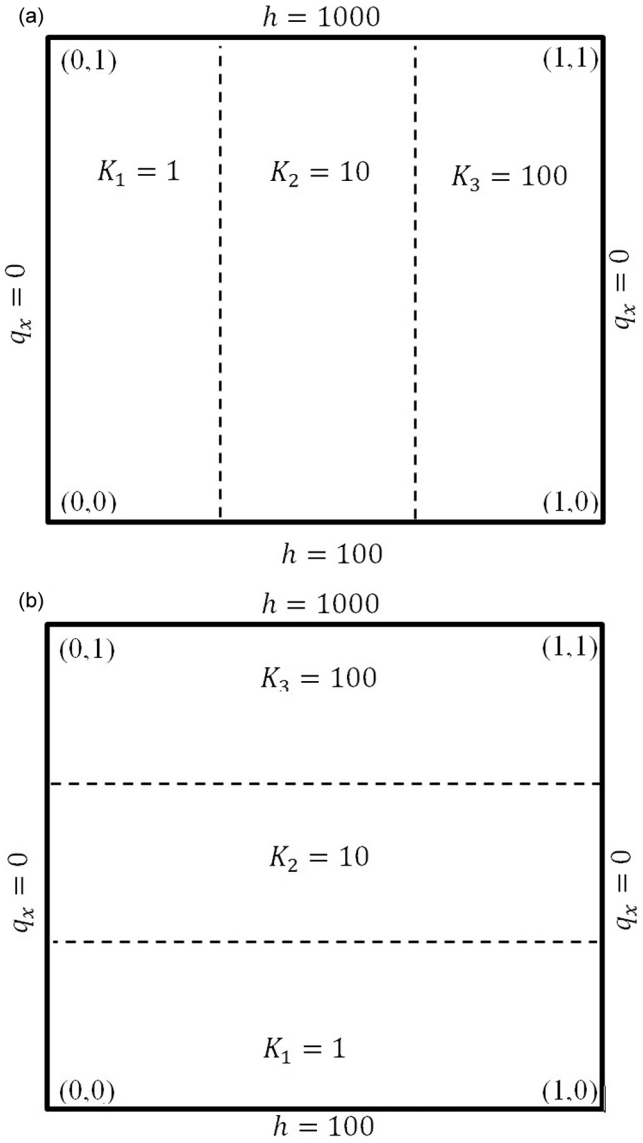

Figure 7. Three hydrofacies zones: (a) parallel stratification and (b) perpendicular stratification. The true K values for the zones are shown.

5.2.3. Flow Perpendicular to Stratification

[37] When flow is perpendicular to stratification and zones are of equal thickness (Figure 7b), the analytic equivalent K is the harmonic mean. The same BCs as in the previous example are used. The same 18 heads are sampled from the FDM solution. A flow rate Q_x is sampled at $x = 0.5$, crossing all zones. The analytic equivalent K of this model is the harmonic mean $\frac{3}{\sum_{j=1}^{m} \frac{1}{K_{(j)}}} = 2.7$. Compared to the previous example, convergence of the direct method is slower, which is likely due to the more complex head profile. Given the same random error (std = 13 or ±3% of the total variation), we find K = 1.6 (10 × 10) and 1.8 (30 × 30). When the error is increased (std = 40 or ±10% error), K = 1.6 (10 × 10) and 1.77 (30 × 30). Although the errors are higher, the method is stable and the estimated K values appear to approach the harmonic mean with grid refinement.

[38] In the above cases, the domain is represented by a single K. To satisfy the governing equation and continuity of the head and flux across the problem domain, the set of equations formulated by the direct method naturally leads to an equivalent K value. The examples are of simple configuration where equivalent K can be obtained analytically, and we anticipate that the results should be applicable to more general settings. Since all these cases do not involve pumping tests, the direct method may serve as a fast and robust tool for evaluating large-scale formation equivalent conductivity without aquifer stimulation.

5.3. Heterogeneous Isotropic Aquifer

[39] The algorithm of section 4.2 is tested by examining 2 unit square models, each with 2 hydrofacies (Figure 8). Prior information with respect to K is specified by equation (18). The same BCs as in Figure 4 are used.

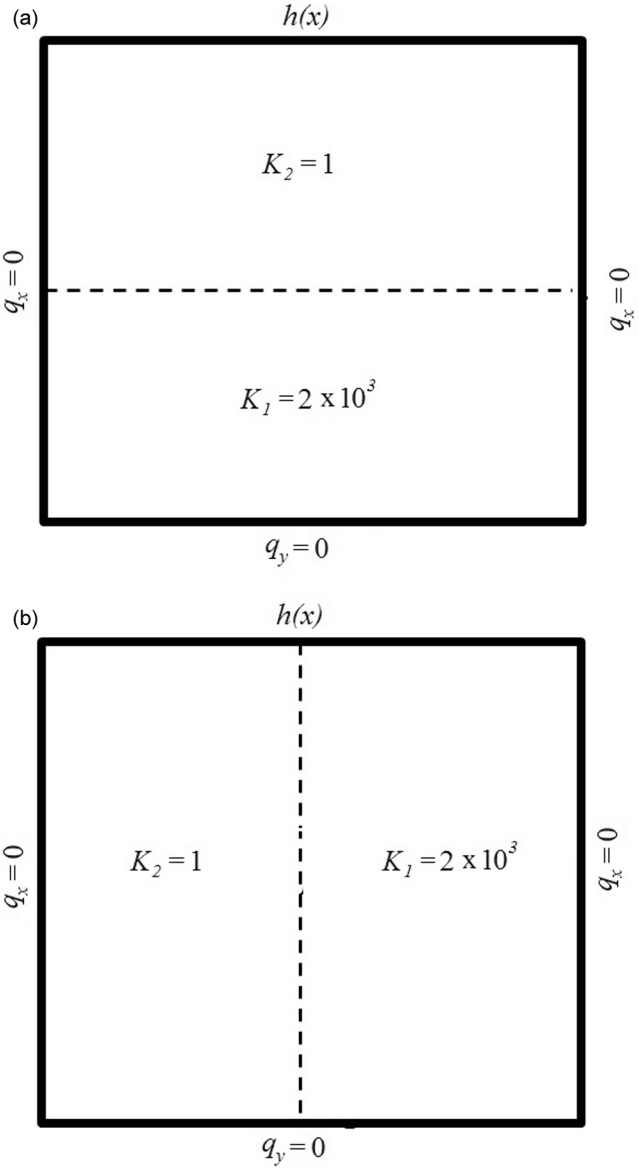

Figure 8. A unit square domain with (a) two vertical zones and (b) two horizontal zones. In both models, BC is described by Figure 4.

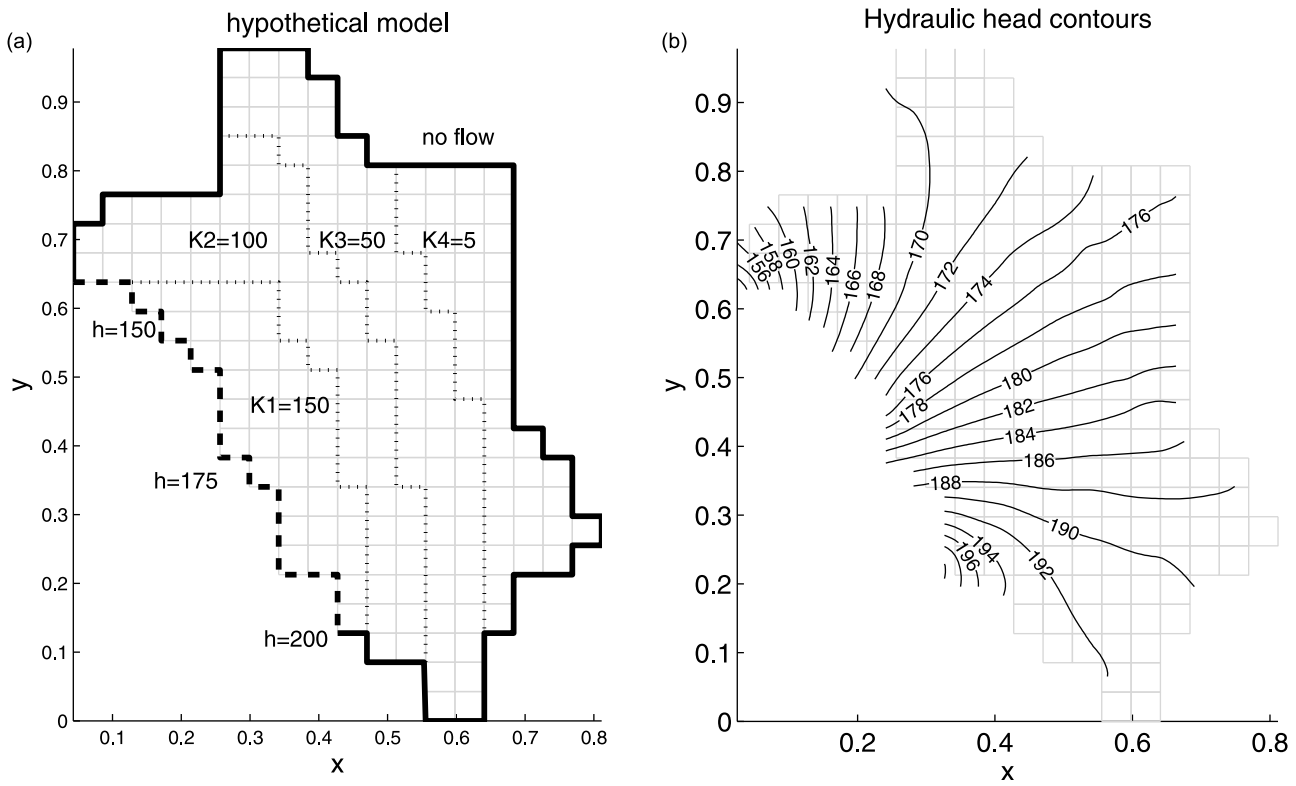

Figure 9. (a) A hypothetical model with four hydrofacies zones. (b) The FDM solution of the hydraulic head for the given conductivities and boundary conditions of Figure 9a.

[40] The horizontally zoned model is tested with 15 observations of heads (x = 0.05, 0.47, 0.9 with 5 heads uniformly placed across each profile) and one flow rate Q_y at x = 1 (Figure 8a). The observation data are sampled from a FDM solution with $K_1 = 2 \times 10^3$ and $K_2 = 1$. Errors are randomly sampled with a *std* = 9.8 (head error $\sim\pm1\%$ of total head variation). Prior information gives $n_g = 2000$. A 10×10 grid results in $K_1 = 1.51 \times 10^3$ and $K_2 = 0.75$ with $\bar{\varepsilon} = 0.34\%$ and $|\varepsilon_{\max}| = 5.4\%$. In a 30×30 grid, $K_1 = 1.86 \times 10^3$ and $K_2 = 0.93$ with $\bar{\varepsilon} = 0.14\%$ and $|\varepsilon_{\max}| = 4\%$.

[41] The vertically zoned model is tested with 24 head observations (x = 0.05, 0.36, 0.68, 0.9) and one flow rate Q_y at x = 1 (Figure 8b). The true conductivities are $K_1 = 2 \times 10^3$ and $K_2 = 1$. Observations errors are the same as in the previous example. The same prior model is used, yielding $K_1 = 1.66 \times 10^3$ and $K_2 = 0.83$ (10×10), and $K_1 = 2.2 \times 10^3$ and $K_2 = 1.1$ (30×30). In both of these zoned models, the correct BCs are recovered; the accuracy in its reconstruction increases with increasing number of elements.

5.4. A Hypothetical Example With Irregular Aquifer Geometry

[42] A hypothetical example with irregular aquifer geometry containing 4 zones is analyzed (Figure 9a), which is a modification of an example from *Heidari and Ranjithan* [1998]. The model consists of a no flow boundary (solid line) and a specified head boundary (dashed line; specified heads shown). Four zones are shown with $K_1 = 150$, $K_2 = 100$, $K_3 = 50$ and $K_4 = 5$. For the given BC, the FDM solution is shown in Figure 9b. To estimate the conductivities and BCs with the direct method, 6 cases are analyzed: the first three utilize 40 observations of hydraulic head and one flow rate, with data error of 0%, 0.5% and 1% (i.e., observed and true heads deviate by 0, $\sim$1 and $\sim$2); the other three utilize 12 observations of hydraulic head and one flow rate with the same increasing data errors. For the error of 0.5%, the reconstruction results, given dense versus sparse observation data, are shown in Figure 10. Overall, the heads are reconstructed reasonably well, the denser observation data giving rise to greater accuracy. The worst results occur near the northeastern corner of the model (Figure 10b), which is believed to be due to a combination of sparse data and the corner location. To evaluate how well the boundary condition is recovered, we plotted hydraulic heads along the entire model boundary for all models and at all error levels. When the data are dense, BC recovery is quite good, with a deviation from true BCs generally increasing with the magnitude of the data error (Figure 11); when the data are sparse, BC errors are greater in comparison, and also increase with the magnitude of the data error (Figure 12). Finally, estimated hydraulic conductivities for the 6 cases are shown in Table 1. Without data error, dense and sparse observations yield very accurate K values. Given the same observation data, accuracy in K estimation degrades with increasing magnitude of the data error, as expected. Overall, K recovery is excellent.

6. Element Shape, Collocation Points, and Error Weighting

[43] Since the Trefftz method is insensitive to mesh distortion [*Jirousek and Zielinski*, 1997], there is no special requirement in the direct method for the element shape and the aspect ratio. Unlike the FEM or FDM, the direct formulations are not based on nodes/vortexes, thus the elements

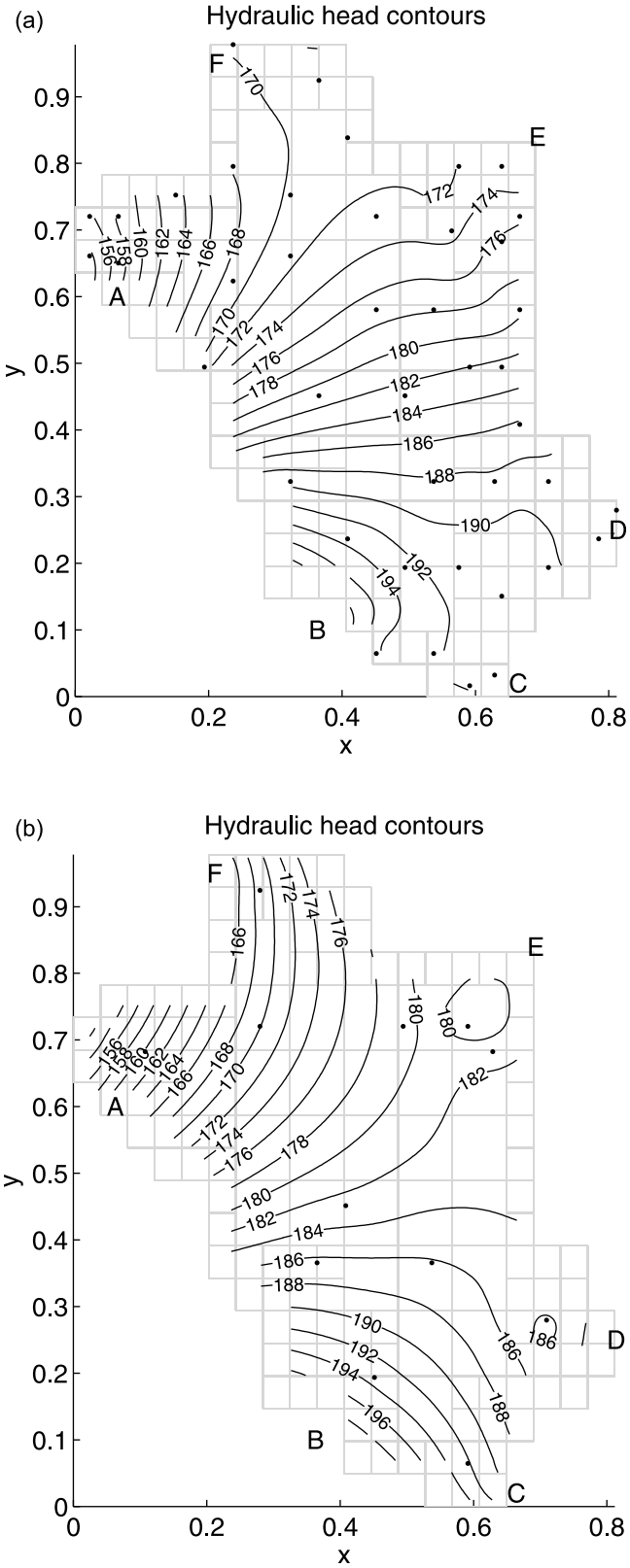

Figure 10. Reconstructed hydraulic heads given (a) 40 and (b) 12 head observations. Locations of head data are shown by dots. A 0.5% error is imposed on each observed head, corresponding to head variation of ±1. Both models use the same single flow rate measurement.

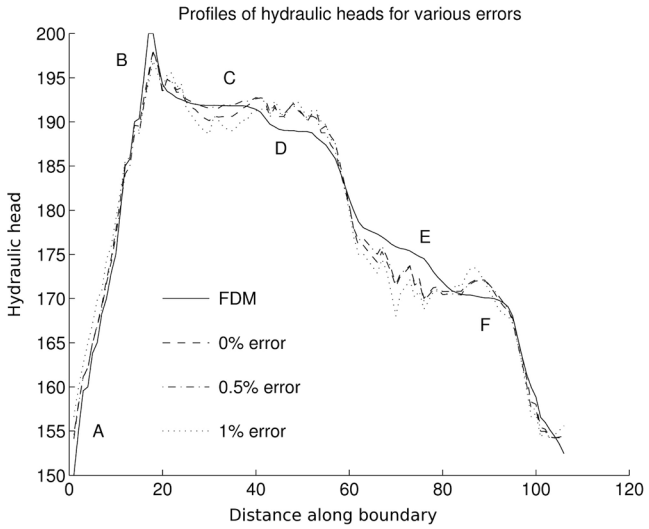

Figure 11. Reconstructed heads along the model boundary (A→F; see Figure 10) for the case with 40 observed heads (head locations shown in Figure 10a).

do not need to meet at the nodes. Though square elements are used here, previous applications of the method in geophysical inversion yielded excellent results with other element shapes [*Irsa*, 2011].

[44] For a regular 2-D domain with uniform rectangular elements, the number of collocation points is $m = \frac{ijc_1}{c_2[2ij - i - j]}$. i is the number of cells across x; j is the number of cells across y; c_1 is the number of unknown coefficients in each element; c_2 is the number of continuity equations. Here, with 5 unknowns in each element and 3 continuity equations, $m \approx 1$. Should one solve a forward BVP problem with the direct method, $m = 1$ is sufficient to provide a unique solution. For the inverse problems, however, one collocation point cannot guarantee a stable solution, thus $m \geq 2$. In all the above examples, we set $m = 2$ and the

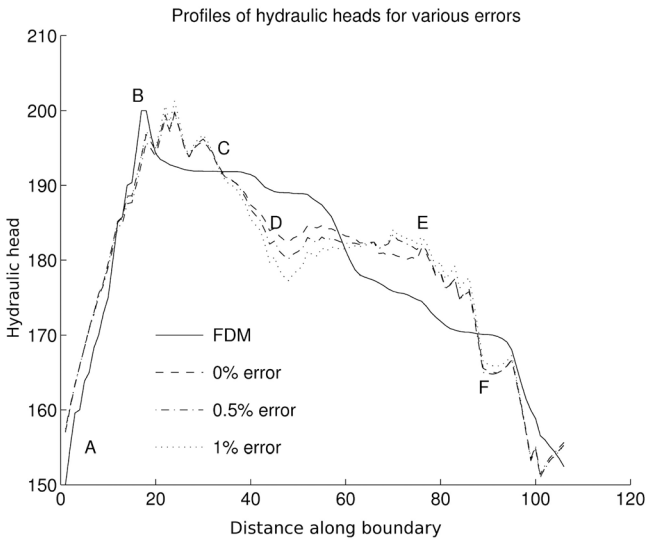

Figure 12. Reconstructed heads along the model boundary (A→F; see Figure 10) for the case with 12 observed heads (head locations shown in Figure 10b).

Table 1. Conductivity Estimated for Different Observation Densities and at Different Levels of Head Measurement Errors[a]

Head Measurement Error	40 Observed Heads				12 Observed Heads			
	K_1	K_2	K_3	K_4	K_1	K_2	K_3	K_4
0% (0)	150	100	50	5	150.22	100.14	50.07	5.01
0.5% (±1)	153.24	102.16	51.08	5.11	159.11	106.07	53.04	5.30
1% (±2)	141.10	94.07	47.03	4.70	161.91	107.94	53.97	5.40

[a]The true conductivities used in the FDM are $K_1 = 150$, $K_2 = 100$, $K_3 = 50$, and $K_4 = 5$.

weighting function on the continuity equations at the collocation points are reduced to 0.5 to account for the fact that $r \cong 2s$ (coefficients defined in equation (16)).

[45] Higher number of collocation points ($m \gg 1$), however, serves as a smoothing parameter which is only preferable if observations are known to contain extremely high errors, such as in an example presented in 5.1.3 where the solution leads to a flow pattern with singularities. Higher m puts more emphasis on the smoothness/continuity of the solution; the observed data are accordingly given lower weights reflecting their high errors. Thus, increasing m is encouraged only if the observation errors are extremely high. In this case, the convergence of the direct method with grid refinement should also be tested. This can be illustrated for a given problem with a true K of 1, where the estimated K does not converge toward 1.0 with increasing number of collocation points (Figure 13). This is true for when the observations contain either no error or very high errors.

[46] The direct method uses head and flux approximation functions that satisfy the governing equation, thus inclusion of the weighting functions, $\delta(p_j - \varepsilon)$, is not necessary. The least squares solution method automatically finds an optimal solution whether the approximation functions are weighted or not. Should the measurement error be known for each observed datum, a user-specified variance can be used. Here a Gaussian noise is assumed, though other distributions can be used. The error variance is the basis upon which weights are assigned to the observed data in the direct formulations. Here the errors are assumed to be uncorrelated, corresponding to the diagonal weight matrix of *Hill and Tiedeman* [2007], though future work may explore correlated errors. For a discussion of how weights can be determined for different hydrogeological data, see *Hill and Tiedeman* [2007].

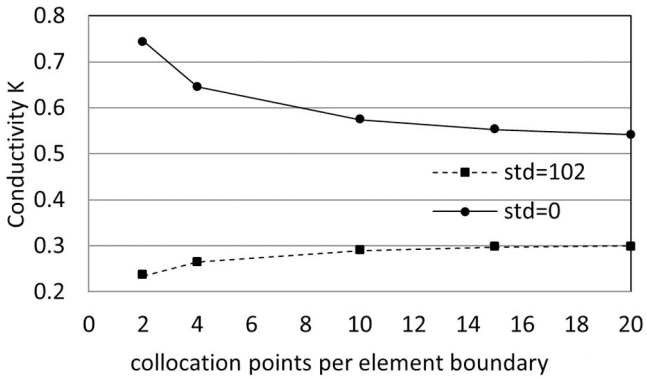

Figure 13. Estimated K versus number of collocation points. Here the problem presented in Figure 4 (sections 5.1.2 and 5.1.3) is solved. Data are 15 heads and 1 flow rate. The true $K = 1$. Std is the standard deviation of the head measurement error.

7. Discussion

[47] A chief strength of the new direct method is that it does not require prior knowledge of the BCs. Also, the model domain does not have to conform to physical boundaries, which are often uncertain or unknown. For example, the model domain can extend into regions where the aquifer does not exist. This will not create unrealistic outcomes; rather, the solution in this area will be an extrapolation of the direct solution constrained by the observed data where they exist, while satisfying the governing equations. Given other physical constraints, the actual boundary conditions can be inferred [*Irsa*, 2011]. On the other hand, the nature of the BCs can be inferred if the observed data are sufficiently dense and accurate (e.g., Figure 5b). Though an locally isotropic aquifer is analyzed here, the method can be extended to locally anisotropic systems with arbitrary conductivity principal orientations via coordinate transform techniques [*Fitts*, 2010].

[48] The new method, due to its low demand on data and robustness in the presence of measurement errors, can be developed into an efficient prototyping tool as part of a field reconnaissance study, before conducting pumping tests and collecting additional data to build detailed models. The inferred BCs can help delineate BVP domains, whereas the conductivity estimates can provide prior information for solving indirect inverse problems using regularized inversion. Although we have shown 2-D results here, extension of the method to 3-D is straightforward using 3-D harmonic approximating functions and 3-D elements with collocation points on its sides [*Irsa and Galybin*, 2010].

[49] Due to its efficiency and flexibility, we envision future extension of this technique to the simultaneous identification of parameter structure, value, state variables, and boundary conditions, up to three dimensions. To incorporate hydrogeological site static data, a variety of geostatistically based iterative schemes (e.g., gradual deformation, sequential self-calibration, soft data integration) can be adapted, where the direct method will replace the "inversion filter" which is typically based on indirect inverse method. Parsimony in parameter structure can be explored using techniques such as data-driven zonation [*Eppstein and Dougherty*, 1996] and penalized objective function/model ranking statistics [*Poeter and Anderson*, 2005]. Though the current method does not incorporate uncertainty measures, uncertainty of the estimated parameters (and possibly boundary conditions) is strongly influenced by material zonation and the prior information equations. By setting additional criteria (e.g., objective function), iterative schemes can be developed to identify alternatively viable parameters, structures, and model boundary conditions. Experimentally, the direct method can be verified in sand tanks, comparing its merits for parameter and BCs estimation against those based on pumping tests and other aquifer characterization techniques.

8. Conclusion

[50] We propose a new direct inverse method for parameter and boundary condition estimation for steady state groundwater flow problems. Its key strength lies in its

computational efficiency, as there is no need to fit an objective function, nor repeated forward simulations of a BVP. We employ a discretization scheme using Trefftz-based approximations and a collocation technique to enforce the global flow solution. The noisy observation data are directly incorporated into the solution matrix, which is solved in a one-step procedure. The output is zoned hydrofacies hydraulic conductivity and analytical expressions of heads and fluxes which can be back substituted to determine the model boundary conditions. Two methods are proposed, one for a homogeneous isotropic aquifer, which can also be used for estimating an equivalent conductivity. The second method is for heterogeneous aquifers where hydrofacies zonation is known in advance, together with prior information on hydraulic conductivity. The direct methods are tested using different data distributions, sampling density, and measurement error variances (up to $\pm 10\%$ of the total variation). Different hydrofacies patterns and heterogeneity variances are tested for both regular and irregular problem domains. All the examples tested were free from instability and conductivity converges with further refining of the grid toward the true or expected values. Under natural flow (i.e., no pumping), the direct method yields an equivalent conductivity of the aquifer, suggesting that the method can be used as an inexpensive characterization tool with which both aquifer parameters and aquifer boundary conditions can be inferred.

[51] **Acknowledgment.** The authors would like to acknowledge the Center for Fundamentals of Subsurface Flow at the School of Energy Resources at the University of Wyoming (WYDEQ49811ZHNG) for the financial support and NSF CI-WATER: Cyberinfrastructure to Advance High Performance Water Resource Modeling for the support.

References

Anderman, E. R., M. C. Hill, and E. P. Poeter (1996), Two-dimensional advective transport in groundwater flow parameter estimation, *Ground Water*, *34*(6), 1001–1009, doi:10.1111/j.1745-6584.1996.tb02165.x.

Anderson, M. P. (2005), Heat as a groundwater tracer, *Ground Water*, *43*(6), 951–968, doi:10.1111/j.1745-6584.2005.00052.x.

Asefa, T., M. W. Kemblowski, G. Urroz, M. McKee, and A. Khalil (2004), Support vectors–based groundwater head observation networks design, *Water Resour. Res.*, *40*, W11509, doi:10.1029/2004WR003304.

Bayless, E. R., A. M. Wayne, and J. R. Ursic (2011), Accuracy of flowmeters measuring horizontal groundwater flow in an unconsolidated aquifer simulator, *Ground Water Monit. Rem.*, *31*(2), 48–62, doi:10.1111/j.1745-6592.2010.01324.x.

Bravo, H. R., F. Jiang, and R. J. Hunt (2002), Using groundwater temperature data to constrain parameter estimation in a groundwater flow model of a wetland system, *Water Resour. Res.*, *38*(8), 1153, doi:10.1029/2000WR000172.

Camporese, M., G. Cassiani, R. Deiana, and P. Salandin (2011), Assessment of local hydraulic properties from electrical resistivity tomography monitoring of a three-dimensional synthetic tracer test experiment, *Water Resour. Res.*, *47*, W12508, doi:10.1029/2011WR010528.

Capilla, J. E., J. J. Gomez-Hernandez, and A. Sahuquillo (1997), Stochastic simulation of transmissivity fields conditional to both transmissivity and piezometric data. 2. Demonstration on a synthetic aquifer, *J. Hydrol.*, *203*(1–4), 175–188, doi:10.1016/S0022-1694(97)00097-8.

Carrera, J., and S. P. Neuman (1986a), Estimation of aquifer parameters under transient and steady state conditions: 1. Maximum likelihood method incorporating prior information, *Water Resour. Res.*, *22*(2), 199–210, doi:10.1029/WR022i002p00199.

Carrera, J., and S. P. Neuman (1986b), Estimation of aquifer parameters under transient and steady state conditions: 2. Uniqueness, stability, and solution algorithms, *Water Resour. Res.*, *22*(2), 211–227, doi:10.1029/WR022i002p00211.

Carrera, J., A. Alcolea, A. Medina, J. Hidalgo, and L. Slooten (2005), Inverse problem in hydrogeology, *Hydrogeol. J.*, *13*, 206–222, doi:10.1007/s10040-004-0404-7.

Chen, Y., and D. Zhang (2006), Data assimilation for transient flow in geologic formations via ensemble Kalman filter, *Adv. Water Resour.*, *29*, 1107–1122, doi:10.1016/j.advwatres.2005.09.007.

Cooley, R. L. (1982), Incorporation of prior information on parameters into nonlinear regression of groundwater flow models: 1. Theory, *Water Resour. Res.*, *18*(4), 965–976, doi:10.1029/WR018i004p00965.

Cooley, R. L. (1983), Incorporation of prior information on parameters into nonlinear regression of groundwater flow models: 2. Applications, *Water Resour. Res.*, *19*(3), 662–676, doi:10.1029/WR019i003p00662.

Day-Lewis, F., J. W. Lane, and S. M. Gorelick (2006), Combined interpretation of radar, hydraulic, and tracer data from a fractured-rock aquifer, *Hydrogeol. J.*, *14*(1–2), 1–14, doi:10.1007/s10040-004-0372-y.

de Marsily, G., J. P. Delhomme, and A. M. Lavenue (2000), Four decades of inverse problems in hydrogeology, *Spec. Pap. Geol. Soc. Am.*, *348*, 1–17.

Delhomme, J. P. (1978), Kriging in the hydrosciences, *Adv. Water Resour.*, *1*(5), 251–266, doi:10.1016/0309-1708(78)90039-8.

Devlin, J. F., P. C. Schillig, I. Bowen, C. E. Critchley, D. L. Rudolph, N. R. Thomson, G. P. Tsoflias, and J. A. Roberts (2012), Applications and implications of direct groundwater velocity measurement at the centimetre scale, *J. Contam. Hydrol.*, *127*, 3–14, doi:10.1016/j.jconhyd.2011.06.007.

Doherty, J., and D. Welter (2010), A short exploration of structure noise, *Water Resour. Res.*, *46*, W05525, doi:10.1029/2009WR008377.

Eppstein, M. J., and D. E. Dougherty (1996), Simultaneous estimation of transmissivity values and zonation, *Water Resour. Res.*, *32*(11), 3321–3336, doi:10.1029/96WR02283.

Fitts, C. R. (2010), Modeling aquifer systems with analytic elements and subdomains, *Water Resour. Res.*, *46*, W07521, doi:10.1029/2009WR008331.

Frind, E. O., and G. F. Pinder (1973), Galerkin solution of the inverse problem for aquifer transmissibility, *Water Resour. Res.*, *9*(5), 1397–1410, doi:10.1029/WR009i005p01397.

Gailey, R. M., A. S. Crowe, and S. M. Gorelick (1991), Coupled process parameter estimation and prediction uncertainty using hydraulic head and concentration data, *Adv. Water Resour.*, *14*(5), 301–314, doi:10.1016/0309-1708(91)90041-L.

Galybin, A. N., and J. Irsa (2010), On reconstruction of three-dimensional harmonic functions from discrete data, *Proc. R. Soc. London, Ser. A*, *466*, 1935–1955, doi:10.1098/rspa.2009.0471.

Galybin, A. N., and S. A. Mukhamediev (2004), Determination of elastic stresses from discrete data on stress orientations, *Int. J. Solids Struct.*, *41*(18–19), 5125–5142, doi:10.1016/j.ijsolstr.2004.04.007.

Ginn, T. R., and J. H. Cushman (1990), Inverse methods for subsurface flow: A critical review of stochastic techniques, *Stochastic Hydrol. Hydraul.*, *4*(1), 1–26, doi:10.1007/BF01547729.

Heidari, M., and R. Ranjithan (1998), A hybrid optimization approach to the estimation of distributed parameters in two-dimensional confined aquifers, *J. Am. Water Resour. Assoc.*, *34*(4), 909–920, doi:10.1111/j.1752-1688.1998.tb01525.x.

Herrera, I. (2000), Trefftz method: A general theory, *Numer. Methods Partial Differ. Equations*, *16*(6), 561–580, doi:10.1002/1098-2426(200011)16:6<561::AID-NUM4>3.0.CO;2-V.

Hill, M. C., and C. R. Tiedeman (2007), *Effective Groundwater Model Calibration: With Analysis of Data, Sensitivities, Predictions, and Uncertainty*, Wiley-Interscience, Hoboken, N. J.

Hunt, R. J., J. Doherty, and M. J. Tonkin (2007), Are models too simple? Arguments for increased parameterization, *Ground Water*, *45*(3), 254–262, doi:10.1111/j.1745-6584.2007.00316.x.

Hyndman, D. W., J. M. Harris, and S. M. Gorelick (1994), Coupled seismic and tracer test inversion for aquifer property characterization, *Water Resour. Res.*, *30*(7), 1965–1977, doi:10.1029/94WR00950.

Irsa, J. (2011), Stress trajectories element method and its modifications for potential problems reconstruction, PhD thesis, Wessex Inst. of Technol., Univ. of Wales, Ashurst, U. K.

Irsa, J., and A. N. Galybin (2009), Heat flux reconstruction in the grinding process from temperature data, in *Proceedings of Computational Methods and Experimental Measurements 14*, pp. 413–423, WIT Press, Southampton.

Irsa, J., and A. N. Galybin (2010), Stress trajectories element method for stress determination from discrete data on principal directions, *Eng. Anal. Boundary Elem.*, *34*, 423–432, doi:10.1016/j.enganabound.2009.12.004.

Irsa, J., and A. N. Galybin (2011a), Numerical reconstruction of 2D potential fields from discrete measurements, *Int. J. Numer. Methods Heat Fluid Flow*, *21*(7), 884–902, doi:10.1108/09615531111162846.

Irsa, J., and A. N. Galybin (2011b), On STEM modeling of tectonic stress field in tsunamigenic regions, *WIT Trans. Modell. Simul.*, *55*, 203–214.

Janssen, G. M. C. M., J. R. Valstar, and A. E. A. T. M. van der Zee (2008), Measurement network design including traveltime determinations to minimize model prediction uncertainty, *Water Resour. Res.*, *44*, W02405, doi:10.1029/2006WR005462.

Jirousek, J., and A. P. Zielinski (1997), Survey of Trefftz-type element formulations, *Comput. Struct.*, *63*(2), 225–242, doi:10.1016/S0045-7949(96)00366-5.

Keating, E. H., J. Doherty, J. A. Vrugt, and Q. Kang (2010), Optimization and uncertainty assessment of strongly nonlinear groundwater models with high parameter dimensionality, *Water Resour. Res.*, *46*, W10517, doi:10.1029/2009WR008584.

Kita, E., and N. Kamiya (1995), Trefftz method: An overview, *Adv. Eng. Software*, *24*, 3–12, doi:10.1016/0965-9978(95)00067-4.

Kitanidis, P. K. (2012), Generalized priors in Bayesian inversion problems, *Adv. Water Resour.*, *36*, 3–10.

Kleinecke, D. (1971), Use of linear programing for estimating geohydrologic parameters of groundwater basins, *Water Resour. Res.*, *7*(2), 367–374, doi:10.1029/WR007i002p00367.

Kolodziej, J. A., and A. P. Zielinski (2009), *Boundary Collocation Techniques and Their Application in Engineering*, WIT Press, Southampton, U. K.

Kupradze, V. D., and M. A. Aleksidze (1964), The method of functional equations for the approximate solution of certain boundary value problems, *USSR Comput. Methods Math. Phys.*, *4*, 82–126, doi:10.1016/0041-5553(64)90006-0.

Leap, D. I., and P. G. Kaplan (1988), A single-well tracing method for estimating regional advective velocity in a confined aquifer: Theory and preliminary laboratory verification, *Water Resour. Res.*, *24*(7), 993–998, doi:10.1029/WR024i007p00993.

Li, Z. C., T. T. Lu, H. Y. Hu, and A. H. D. Cheng (2008), *Trefftz and Collocation Methods*, WIT Press, Southampton, U. K.

Li, Z.-C., L.-J. Young, H.-T. Huang, Y.-P. Liu, and A. H. D. Cheng (2010), Comparisons of fundamental solutions and particular solutions for Trefftz methods, *Eng. Anal. Boundary Elem.*, *34*(3), 248–258, doi:10.1016/j.enganabound.2009.10.001.

Liu, G., Y. Chen, and D. Zhang (2008), Investigation of flow and transport processes at the MADE site using ensemble Kalman filter, *Adv. Water Resour.*, *31*, 975–986, doi:10.1016/j.advwatres.2008.03.006.

Liu, X., and P. K. Kitanidis (2011), Large-scale inverse modeling with an application in hydraulic tomography, *Water Resour. Res.*, *47*, W02501, doi:10.1029/2010WR009144.

Maunder, E. A. W. (2003), Trefftz in translation, *Comput. Assisted Mech. Eng. Sci.*, *10*, 545–563.

McKenna, S. A., and E. P. Poeter (1995), Field example of data fusion in site characterization, *Water Resour. Res.*, *31*(12), 3229–3240, doi:10.1029/95WR02573.

McLaughlin, D., and L. R. Townley (1996), A reassessment of the groundwater inverse problem, *Water Resour. Res.*, *32*(5), 1131–1161, doi:10.1029/96WR00160.

Medina, A., and J. Carrera (1996), Coupled estimation of flow and solute transport parameters, *Water Resour. Res.*, *32*(10), 3063–3076, doi:10.1029/96WR00754.

Morshed, J., and J. J. Kaluarachchi (1998), Parameter estimation using artificial neural network and genetic algorithm for free-product migration and recovery, *Water Resour. Res.*, *34*(5), 1101–1113, doi:10.1029/98WR00006.

Nelson, R. W. (1960), In place measurement of permeability in heterogeneous media: 1. Theory of a proposed method, *J. Geophys. Res.*, *65*, 1753–1760, doi:10.1029/JZ065i006p01753.

Nelson, R. W. (1961), In place measurement of permeability in heterogeneous media: 2. Experimental and computational considerations, *J. Geophys. Res.*, *66*, 2469–2478, doi:10.1029/JZ066i008p02469.

Nelson, R. W. (1968), In place determination of permeability distribution of heterogeneous porous media through analysis of energy dissipation, *Soc. Pet. Eng. J.*, *3*, 33–42.

Neuman, S. P. (1973), Calibration of distributed parameter groundwater flow models viewed as a multiple-objective decision process under uncertainty, *Water Resour. Res.*, *9*(4), 1006–1021, doi:10.1029/WR009i004p01006.

Paige, C. C., and M. A. Saunders (1982), LSQR: An algorithm for sparse linear equations and sparse least squares, *Trans. Math. Software*, *8*(1), 43–71, doi:10.1145/355984.355989.

Poeter, E. P., and D. Anderson (2005), Multimodel ranking and inference in ground water modeling, *Ground Water*, *43*(4), 597–605, doi:10.1111/j.1745-6584.2005.0061.x.

Ronayne, M. J., S. M. Gorelick, and J. Caers (2008), Identifying discrete geologic structures that produce anomalous hydraulic response: An inverse modeling approach, *Water Resour. Res.*, *44*, W08426, doi:10.1029/2007WR006635.

Sagar, B., S. Yakowitz, and L. Duchstein (1975), A direct method for the identification of the parameters of dynamic nonhomogeneous aquifers, *Water Resour. Res.*, *11*(4), 563–570, doi:10.1029/WR011i004p00563.

Sun, N.-Z. (1994), *Inverse Problems in Groundwater Modeling, Theory Appl. Transp. Porous Media*, vol. 6, Kluwer Acad., Dordrecht, Netherlands.

Sun, N.-Z., and W. W.-G. Yeh (1985), Identification of parameter structure in groundwater inverse problem, *Water Resour. Res.*, *21*(6), 869–883, doi:10.1029/WR021i006p00869.

Sun, N.-Z., M. C. Jeng, and W. W.-G. Yeh (1995), A proposed geological parameterization method for parameter identification in three-dimensional groundwater modeling, *Water Resour. Res.*, *31*(1), 89–102, doi:10.1029/94WR02276.

Tonkin, M., and J. Doherty (2009), Calibration-constrained Monte Carlo analysis of highly parameterized models using subspace techniques, *Water Resour. Res.*, *45*, W00B10, doi:10.1029/2007WR006678.

Trefftz, E. (1926), Ein Gegenstück zum Ritzschen Verfahren, in *Proceedings of the 2nd International Congress on Applied Mechanics*, pp. 131–137, Orell Fussli Verlag, Zurich.

Tsou, M.-S., S. P. Perkins, X. Zhan, D. O. Whittemore, and L. Zheng (2006), Inverse approaches with lithologic information for a regional groundwater system in southwest Kansas, *J. Hydrol.*, *318*, 292–300, doi:10.1016/j.jhydrol.2005.06.027.

Vrugt, J. A., P. H. Stauffer, T. Wohling, B. A. Robinson, and V. V. Vesselinov (2008a), Inverse modeling of subsurface flow and transport properties: A review with new developments, *Vadose Zone J.*, *7*, 843–864, doi:10.2136/vzj2007.0078.

Vrugt, J. A., C. J. F. ter Braak, M. P. Clark, J. M. Hyman, and B. A. Robinson (2008b), Treatment of input uncertainty in hydrologic modeling: Doing hydrology backward with Markov chain Monte Carlo simulation, *Water Resour. Res.*, *44*, W00B09, doi:10.1029/2007WR006720.

Wagner, B. J. (1995), Sampling design methods for groundwater modeling under uncertainty, *Water Resour. Res.*, *31*(10), 2581–2591, doi:10.1029/95WR02107.

Wang, M., and C. Zheng (1996), Aquifer parameters estimation under transient and steady-state conditions using genetic algorithms, in *Calibration and Reliability in Groundwater Modeling, Proceedings of the ModelCARE 96 Conference*, *IAHS Publ.*, *237*, 21–30.

Weiss, R., and L. Smith (1998a), Parameter space methods in joint parameter estimation for groundwater flow models, *Water Resour. Res.*, *34*(4), 647–661, doi:10.1029/97WR03467.

Weiss, R., and L. Smith (1998b), Efficient and responsible use of prior information in parameter estimation for groundwater models, *Ground Water*, *36*(1), 151–163, doi:10.1111/j.1745-6584.1998.tb01076.x.

Woodbury, A. D., and L. Smith (1988), Simultaneous inversion of hydrogeologic and thermal data: 2. Incorporation of thermal data, *Water Resour. Res.*, *24*(3), 356–372, doi:10.1029/WR024i003p00356.

Yeh, W. W.-G. (1986), Review of parameter identification procedures in groundwater hydrology: The inverse problem, *Water Resour. Res.*, *22*(2), 95–108, doi:10.1029/WR022i002p00095.

Yeh, W. W.-G., Y. S. Yoon, and K. S. Lee (1983), Aquifer parameter identification with kriging and optimum parametrization, *Water Resour. Res.*, *19*(1), 225–233, doi:10.1029/WR019i001p00225.

Zhu, J. F., and T. C. J. Yeh (2005), Characterization of aquifer heterogeneity using transient hydraulic tomography, *Water Resour. Res.*, *41*, W07028, doi:10.1029/2004WR003790.

Zimmerman, D. A., et al. (1998), A comparison of seven geostatistically based inverse approaches to estimate transmissivities for modeling advective transport by groundwater flow, *Water Resour. Res.*, *34*(6), 1373–1413, doi:10.1029/98WR00003.